Supporting Information (SI) for:

Design and Preparation of Three-Dimensional Hetero-electrocatalysts of NiCo -Layered Double Hydroxide Nanosheets Incorporated with Silver Nanoclusters for Enhanced Oxygen Evolution Reactions

Bingxian Chu [#a],Qiuxia Ma [#a], Zesheng Li[c],Bolin Li [#a], Furong Huang[a], Qi Pang[a*], Yibo Chen[b*],Bin Li[a], Jin Zhong Zhang[d]*

[a] School of Chemistry and Chemical Engineering Guangxi University / Guangxi Key Laboratory of Electrochemical Energy Materials, 100 University Road, Nanning 530004, China

[b]School of Chemistry and Chemical Engineering/Guangzhou Key Laboratory for Clean Energy and Materials, Guangzhou University, Guangzhou 510006, P. R. China

[c] College of Chemistry, Guangdong University of Petrochemical Technology, Maoming, Guangdong 525000, China.

[d]Department of Chemistry and Biochemistry, University of California, Santa Cruz, California 95064, USA

[#]These authors contributed equally to the paper

**Correspondence author: Qi Pang, E-mail address: pqigx@163.com ; Yibo Chen, E-mail: chenyibo@gzhu.edu.cn and Zesheng Li, E-mail: lzs212@163.com*

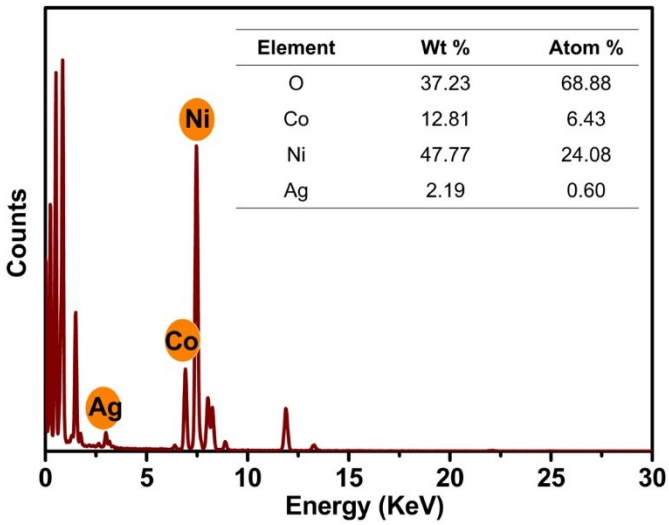

Figure S1. Elemental dispersive X-ray spectroscopy of Ag@NiCo-LDH/NF.

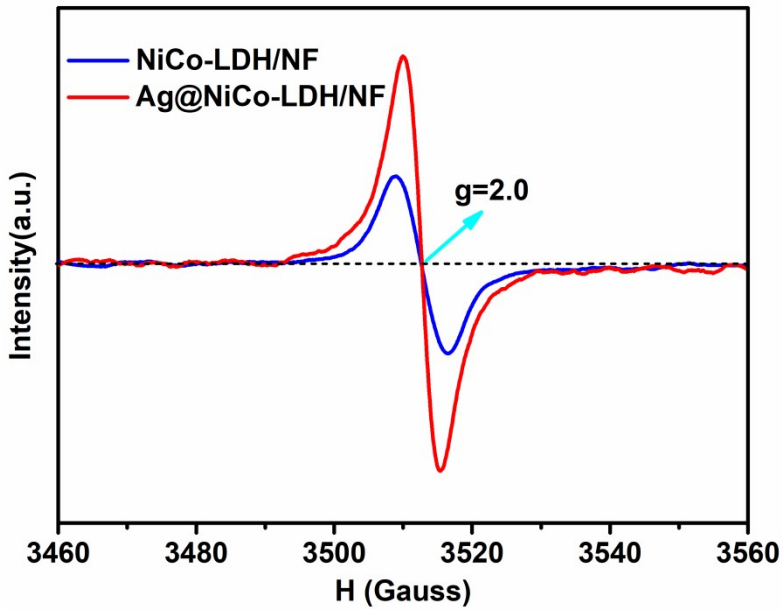

Figure S2. EPR spectra analysis of NiCo-LDH/NF and Ag@NiCo-LDH/NF.

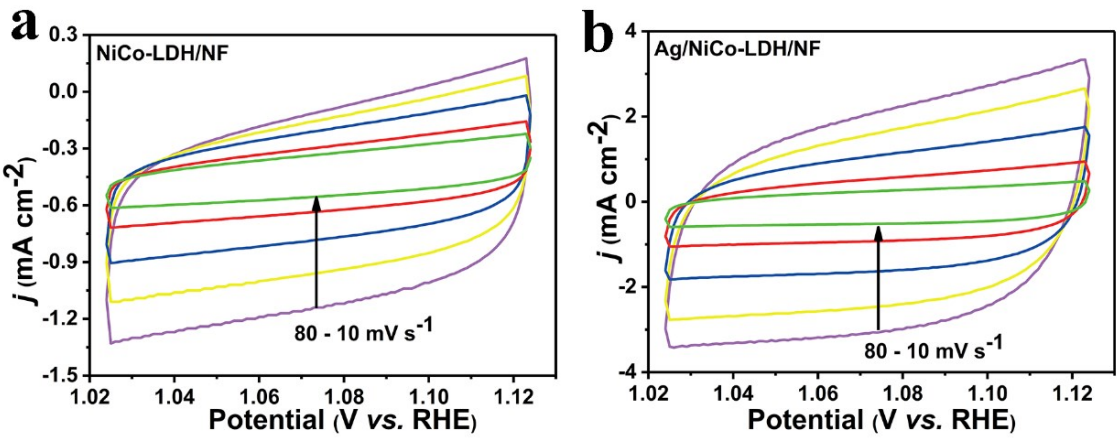

Figure S3. Cyclic voltammograms (CV) at various scan rates for (a) NiCo-LDH/NF; (b) Ag@NiCo-LDH/NF

Table S1. Control samples with different Ag content

Samples	The amount of Ag (mg)	else
Sample-1	5.6	The other conditions remain the same
Sample-2	14.0	
Sample-3	28.0	
Sample-4	42.0	
Sample-5	50.4	

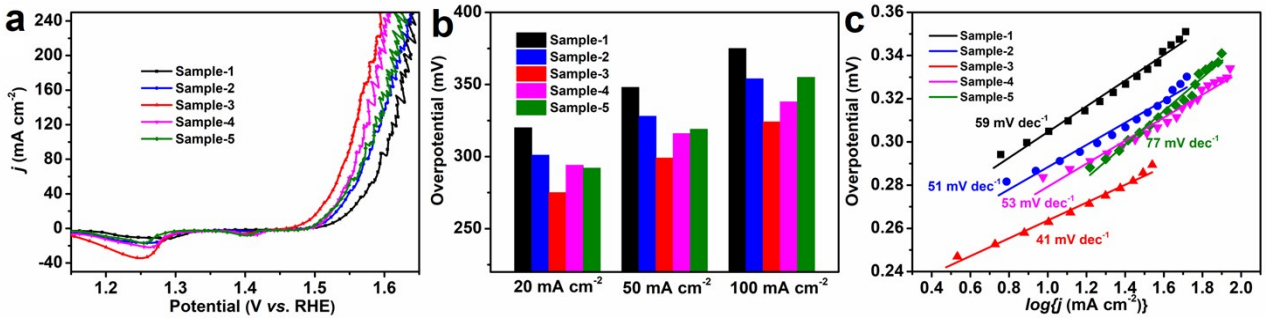

Figure S4. Comparison of electrocatalytic OER of control samples in Table S1: (a) Polarization curves at a scan rate of 5 mV s^{-1} and (b) Overpotential required at different current densities. (c) Tafel plot derived from (a).

Table S2. Electrochemical performance of NiCo-LDH/NF and Ag@NiCo-LDH/NF materials in alkaline solution.

Samples	C_{dl} (mF cm^{-2})	ECSA (cm^{-2})
NiCo-LDH/NF	6	150
Ag@NiCo-LDH/NF	32	800

ECSA= C_{dl}/C_s , Where C_s is the specific capacitance, whose value was reported to be 0.040 mF cm^{-2} in 1.0 M KOH.

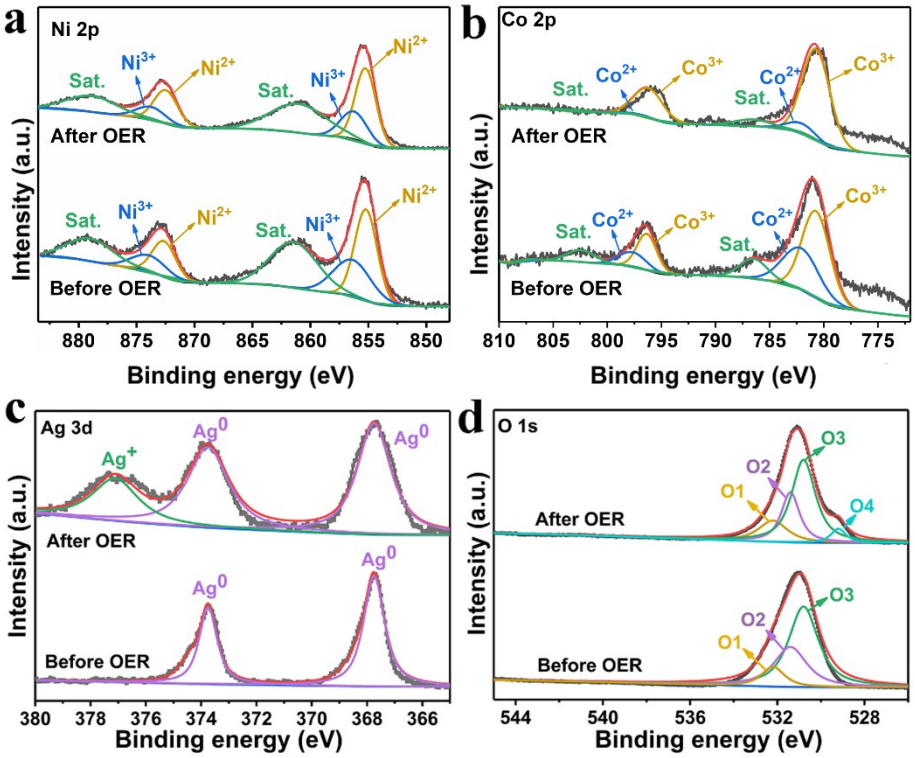

Figure S5. High resolution XPS spectra of (a) Ni 2p, (b) Co 2p, (c) O 1s, and (d) Ag 3d for Ag@NiCo-LDH/NF before and after OER test.

Table S3. Comparison OER activity in 1 M KOH for Ag@NiCo-LDH/NF with other Ni- and Co-based electrocatalysts.

electrocatalyst	**$\eta_{10@OER}$ (mV)**	**Tafel slope (mV dec^{-1})**	**References**
Plasma-Engraved Co_3O_4	300	68	[20]
$(Co_{1-x}Ni_x)(S_{1-y}P_y)_2/G$	285	105	S1
Co-PBA plasma 2h	274	53	S2
NiCoP nanocube	271	85	S3

Ag@NiCo-LDH /NF	262	41	This work
$Ni_{0.83}Fe_{0.17}(OH)_2$	245	61	S4
NiFeSe@NiSe|O@CC	270	63.2	[31]
$Co(OH)_2$ NPs/Co_3O_4 NCs	281	52.7	S5
Co_3O_4/Co-Fe oxide DSNBS	297	61	S6
B-$Ni(OH)_2$	340	43	S7

References

[1] Song, H.J.; Yoon, H.; Ju, B.; et al., 3d Architectures of Quaternary Co-Ni-S-P/Graphene Hybrids as Highly Active and Stable Bifunctional Electrocatalysts for Overall Water Splitting, *Adv. Energy Mater.,* **2018**, 8, 1802319.

[2] Guo, Y.; Wang, T.; Chen, J.; et al., Air Plasma Activation of Catalytic Sites in a Metal-Cyanide Framework for Efficient Oxygen Evolution Reaction, Advanced Energy Materials, *Adv. Energy Mater.,* **2018**, 8, 1800085.

[3] Xuan, C.; Wang, J.; Xia, W.; et al., Porous Structured Ni–Fe–P Nanocubes Derived from a Prussian Blue Analogue as an Electrocatalyst for Efficient Overall Water Splitting, *ACS Appl. Mater. Interfaces*, **2017**, 9, 26134-26142.

[4] Zhou, Q.; Chen, Y.; Zhao, G.; et al., Active-Site-Enriched Iron-Doped Nickel/Cobalt Hydroxide Nanosheets for Enhanced Oxygen Evolution Reaction, *ACS Catal.*, **2018,** 8, 5382-5390.

[5] Xu, H.; Wei, J.; Zhang, M.; et al., Heterogeneous $Co(OH)_2$ Nanoplates/Co_3O_4

Nanocubes Enriched with Oxygen Vacancies Enable Efficient Oxygen Evolution Reaction Electrocatalysis, *Nanoscale*, **2018**, 10, 18468-18472.

[6] Wang, X.; Yu, L.; Guan, B.Y.; et al., Metal-Organic Framework Hybrid-Assisted Formation of Co_3O_4/Co-Fe Oxide Double-Shelled Nanoboxes for Enhanced Oxygen Evolution, *Adv. Mater.*, **2018**, 30, 1801211.

[7] Zhang, Z.; Zhang, T.; Lee, J.Y., Enhancement Effect of Borate Doping on the Oxygen Evolution Activity of A-Nickel Hydroxide, *ACS Appl. Nano Mater.*, **2018**, 1, 751-758.

Theoretical Section

OER involves four electron transfer processes, the four basic steps are as follows:

$$H_2O(l)+*\rightarrow *OH+(H^++e^-) \quad (1)$$

$$*OH\rightarrow *O+(H^++e^-) \quad (2)$$

$$*O+H_2O(l)\rightarrow *OOH+(H^++e^-) \quad (3)$$

$$*OOH\rightarrow *+O_2(g)+ (H^++e^-) \quad (4)$$

* represented the active site on the catalyst surface; *O,*OH,*OOH represented the intermediate species adsorbed on the active sites. The free energy of H^++e^- was substituted by 1/2 $E(H_2)$ under conditions of pH = 0, P = 1 atm, T = 298 K conditions. The formula for calculating OER free energy is as follows: $\Delta G = \Delta E + \Delta ZPE - T\Delta S$. The ΔE can be obtained by computation of geometrical structures. ΔZPE and ΔS are calculated using gas phase of the reactants and products is determined by the vibration frequency and standard table. Assuming that the entropy of the adsorbed

atom/molecule at the surface-active site were assumed to be zero (the gas molecules as show in Table S3), and the dependence of enthalpy on temperature is neglected in the calculation.

Therefore, the free energy of each intermediate species adsorbed could be expressed as follows:

$$\Delta G(*OH)=E(*OH)-E(*)-E_{H_2O}+1/2E_{H_2}+(\Delta ZPE-T\Delta S)_1 \quad (5)$$

$$\Delta G(*O)=E(*O)-E(*OH)+1/2E_{H_2}+(\Delta ZPE-T\Delta S)_2 \quad (6)$$

$$\Delta G(*OOH)=E(*OOH)-E(*O)-E_{H_2O}+1/2E_{H_2}+(\Delta ZPE-T\Delta S)_3 \quad (7)$$

where the E(*), E(*OH), E(*O), E(*OOH) are the total energy calculated by DFT of the pure surface and the adsorbed surfaces with *OH, *O, and *OOH, respectively. E_{H_2O}, E_{H_2} and E_{O_2} are the calculated energies of individual molecules of H_2O, H_2 and O_2, respectively.

The reaction energy of each step is expressed by the free energy of the intermediate, and the effects of PH and an external bias U are represented by the following equation:

$$\Delta G_1=\Delta G(*OH)-\Delta G(H_2O)-eU+k_BT\ln\alpha_{H+} \quad (8)$$

$$\Delta G_2=\Delta G(*O)-\Delta G(*OH)-eU+k_BT\ln\alpha_{H+} \quad (9)$$

$$\Delta G_3=\Delta G(*OOH)-\Delta G(*O)-\Delta G(H_2O)-eU+k_BT\ln\alpha_{H+} \quad (10)$$

$$\Delta G_4=\Delta G(O_2)-\Delta G(*OOH)-eU+k_BT\ln\alpha_{H+} \quad (11)$$

Because all energy is in water as a benchmark, $\Delta G(H_2O)=0$ eV, $\Delta G(O_2)=4.92$ eV(four times the equilibrium potential at the time of water formation, and 1.23 eV under

standard conditions).

The overpotential η is defined:

$\eta = -\max(\Delta G1, \Delta G2, \Delta G3, \Delta G4) - 1.23$ eV

Table S4 The free energy of molecules.

	Pressure /bar	Temperature /K	E(DFT) /eV	DG /eV	G /eV	PH	-0.059*PH
O_2(g)	1.000	298.150			-9.920	14	-0.8288
H_2(g)	1.000	298.150	-6.760	-0.045	-6.800		
H_2O(l)	0.035	298.150	-14.220	-0.001	-14.220		

Table S5 The free energy of NiCo-LDH.

	E/eV	ZPE/eV	G/eV		U=0, PH=0	U=0, PH=0	U=0, PH=14	U=0.401, PH=14
slab	-860.281	0.000	-860.281	$+2H_2O$	-888.721	0.000	0.000	0.000
OH*	-871.004	0.377	-870.628	$+H_2O + 1/2\ H_2$	-888.248	0.473	-0.356	-0.757
O*	-866.841	0.119	-866.722	$+H_2O + H_2$	-887.742	0.978	-0.679	-1.482
OOH*	-875.100	0.450	-874.651	$+ 3/2\ H_2$	-884.851	3.870	1.384	0.180
slab	-860.281	0.000	-860.281	$+ O_2 + 2H_2$	-883.801	4.920	1.605	0.000

Table S6. The free energy of Ag@NiCo-LDH.

	E/eV	ZPE/eV	G/eV		U=0, PH=0	U=0, PH=0	U=0, PH=14	U=0.401, PH=14
slab	-857.732	0.000	-857.732	$+2H_2O$	-886.172	0.000	0.000	0.000
OH*	-868.866	0.336	-868.529	$+H_2O + 1/2\ H_2$	-886.149	0.023	-0.806	-1.207
O*	-864.463	0.096	-864.368	$+H_2O + H_2$	-885.388	0.785	-0.873	-1.675
OOH*	-873.076	0.435	-872.642	$+ 3/2\ H_2$	-882.842	3.331	0.845	-0.359

slab	-857.732	0.000	-857.732	+ O_2 + $2H_2$	-881.252	4.920	1.605	0.000

Table S7. The Crystal Orbital Hamilton Populations for Ag@NiCo-LDH (**Figure 8.** a))

-ICOHP	5s-2s up	5s-2s dw	5s-2p up	5s-2p dw	4d-2s up	4d-2s dw	4d-2p up	4d-2p dw	total
Ag1-O1	0.111	0.128	0.223	0.213	0.005	0.003	0.010	0.025	0.718
Ag1-O2	0.143	0.165	0.256	0.250	0.012	0.011	0.025	0.040	0.902
Ag1-O3	0.144	0.167	0.261	0.254	0.012	0.010	0.028	0.043	0.918
Ag2-O4	0.149	0.158	0.262	0.265	0.009	0.010	0.013	0.044	0.909
Ag2-O5	0.178	0.189	0.302	0.305	0.026	0.029	0.041	0.067	1.135
Ag2-O6	0.183	0.194	0.300	0.302	0.024	0.026	0.041	0.066	1.136

Table S8. The Crystal Orbital Hamilton Populations for NiCo-LDH (**Figure S1**)

-ICOHP	5s-2s up	5s-2s dw	5s-2p up	5s-2p dw	4d-2s up	4d-2s dw	4d-2p up	4d-2p dw	total
Ni-O7	0.205	0.212	0.213	0.214	-0.007	0.063	0.014	0.262	1.176
Ni-O8	0.212	0.215	0.218	0.220	-0.006	0.064	0.015	0.274	1.211
Ni-O9	0.218	0.220	0.218	0.220	-0.006	0.064	0.016	0.274	1.224
Ni-O10	0.226	0.231	0.272	0.270	-0.010	0.065	0.020	0.276	1.351
Ni-O11	0.224	0.228	0.262	0.260	-0.009	0.065	0.019	0.279	1.328
Ni-O12	0.219	0.228	0.255	0.256	-0.010	0.065	0.017	0.265	1.295

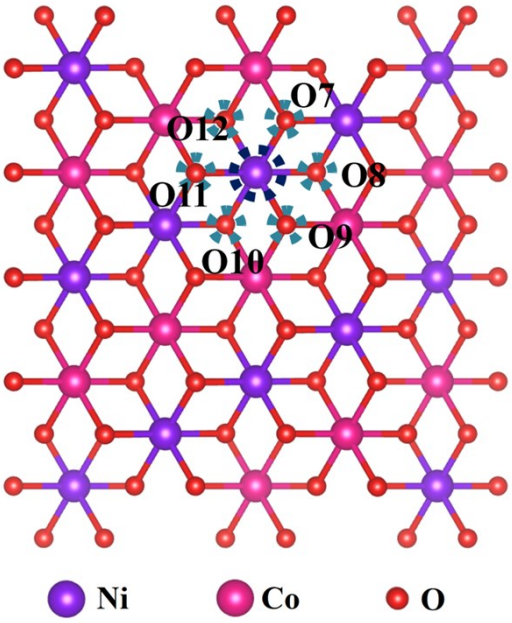

Figure S6. Top view of the crystal model of NiCo-LDH.

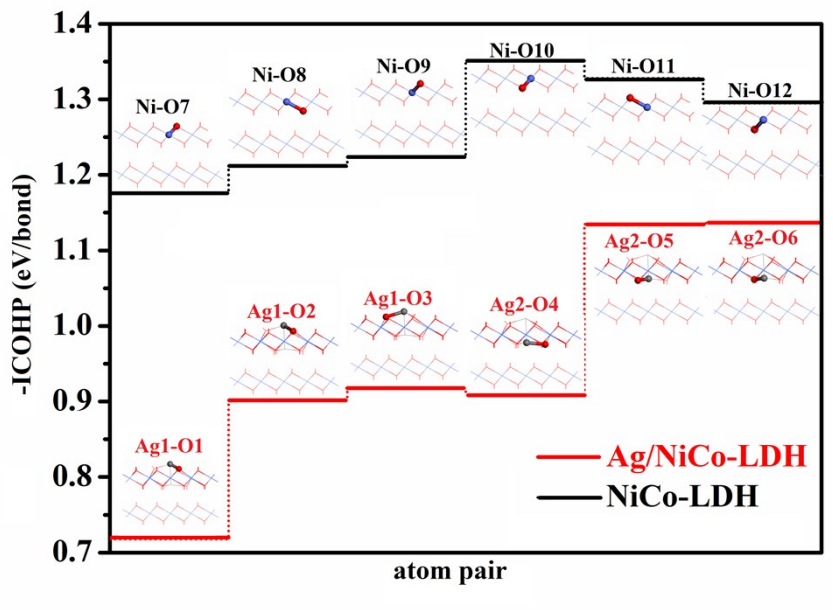

Figure S7.The -ICOHP of NiCo-LDH and Ag@NiCo-LDH.

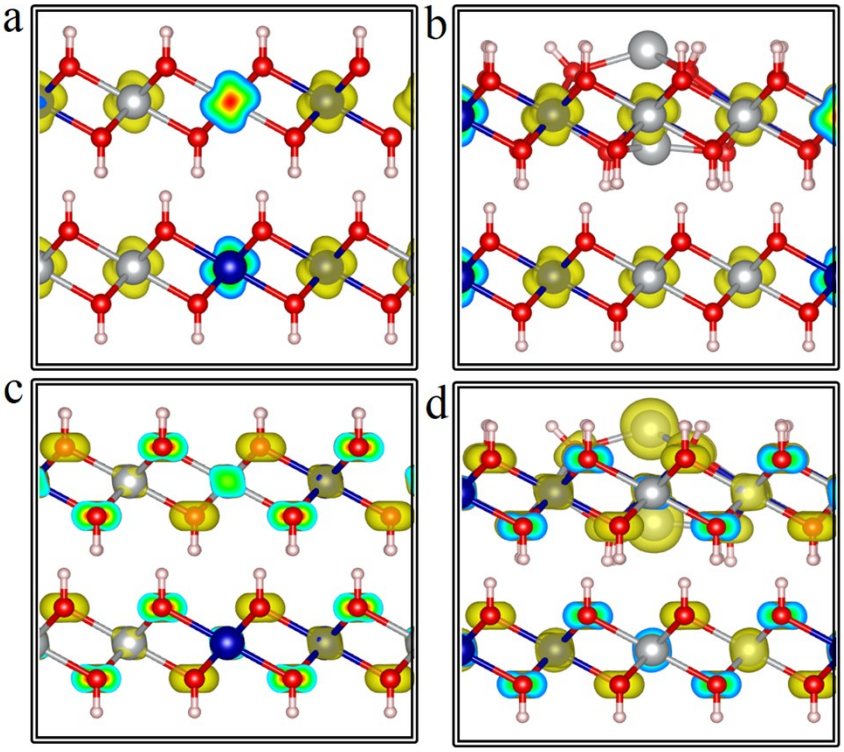

Figure S8. The partial charge density (-0.7~0 eV, isovalue = 0.03 atomic units) of (a) NiCo-LDH and (b) Ag@NiCo-LDH, the partial charge density (-2~-6 eV, isovalue = 0.1 atomic units) of (c) NiCo-LDH and (d) Ag@NiCo-LDH.